Caries Detection in Panoramic Dental X-ray Images

João Oliveira and Hugo Proença

Department of Computer Science, IT - Instituto de Telecomunicações
University of Beira Interior, Covilhã, Portugal

Abstract. Dental Caries, also known as dental decay or tooth decay, is defined as a disease of the hard tissues of the teeth caused by the action of microorganisms found in plaque on fermentable carbohydrates (principally sugars). Therefore, the detection of dental caries in a preliminary stage is an important task. This chapter has two major purposes, firstly to announce the availability of a new data set of panoramic dental X-ray images. This data set contains 1392 images with varying types of noise, usually inherent to this kind of images. Secondly, we present a complete case study for the detection of dental caries in panoramic dental X-ray images.

1 Introduction

Dental Caries, also know as tooth decay, are a preventable disease. Given its dynamic nature, once established, they can be treated or reversed prior to significant cavitation take place. Primary diagnosis involves visual inspection of all the visible tooth surfaces. Dental radiographs (X-rays) may show dental caries before they are visible, particularly caries between the teeth. Large dental caries are usually apparent to the human observer, but smaller lesions can be difficult to detect. Visual and tactile inspections along with radiographs are therefore employed frequently among dentists.

1.1 Dental X-ray

Dental X-rays are pictures of the teeth, bones, and soft tissues around them that help find problems within the teeth, mouth, and jaws. X-ray pictures can show cavities, hidden dental structures, and bone loss that cannot be seen during a visual examination. Dental X-rays may also be done as follow-up after dental treatment. There are three main different types of dental X-ray: bitewing, periapical and panoramic. A full-mouth series of periapical X-rays are most often done during a person's first visit to the dentist. Bitewing X-rays are used during checkups to look for tooth decay. Panoramic X-rays may be used occasionally.

1.2 Main Applications

Automated image analysis processes have been achieving higher relevance for many purposes and the results can be considered satisfactory. In the specific area of medical image processing, the detection of health situations as earliest as possible increases the role of such automated systems.

1.3 Clinical Environments

Dental X-ray images are also used in clinical environments, in the detection and prediction of Bone Mineral Density (BMD) for the diagnosis of osteoporosis. In [11] authors assessed the trabecular pattern of dental X-rays to predict BMD.

In [10] authors proposed a framework to segment dental X-ray images. The segmentation contains two phases: training, in which they manually selected images representative of the whole. These images are segmented based on a hierarchy of regions of detectable "level set". Further features are extracted by Principal Component Analysis (PCA) [9], and feed a Support Vector Machine (SVM) classifier scheme [5][12]. In the segmentation of new data the SVM provides the initial contours corresponding to the possible lesion region.

1.4 Biometrics

In biometrics dental X-ray are used for the identification of deceased individuals [8]. This process is based on the comparison of the Ante-Mortem (AM) and Post-Mortem (PM) dental X-rays. In [4] the tooth contour is extracted for matching purposes of dental radiographs, which is done by the directional snake process [14]. Three main stages are performed; initialization, convergence to the gradient and an adjustment at the end of the process. In the first stage authors initialize the snake, for that the gumline detection is performed. The gumline is the "visual line" that separates the root area from the crown area. The method takes advantage of the fact that there is an intensity increase at the gum lines from the crow area to the root area. The Gradient Vector Flow (GVF) field of the edges detected by the Canny operator is used as the external energy for the convergence gradient stage. In the final stage the fine adjustments are based on the fact that true pixels boundaries always had in their neighbor pixels of lower intensities. The external energy is defined by (1), where $E_{ext,1}$ is the external energy of the teeth boundaries, $E_{ext,2}$ corresponds to the image intensity and ω controls the trade-off between the gradient and the intensity. The results of this paper are quite interesting, but it should be noted that authors simply applied the method to bitewing dental X-ray images, that are much more easier to handle, due to the limited amount of available information.

$$E_{ext} = E_{ext,1} + \omega E_{ext,2} \tag{1}$$

In [3] the matching of dental X-ray images for human identification, is based on the gap valley detection, tooth isolation, contour extraction (crown and root)

and in the contours matching edge. This method is initialized by means of a user interaction, where the user is asked to mark a point between jaws. Further, the horizontal projection of the intensities is calculated, being expected that near this point will be a gap intensity valley. Based on this, using the probability function:

$$p_{v_i}(D_i, y_i) = p_{v_i}(D_i)p_{v_i}(y_i),\qquad(2)$$

where

$$p_{v_i}(D_i) = c(1 - \frac{D_i}{\max_k D_k}),\qquad(3)$$

and

$$p_{v_i}(y_i) = \frac{1}{\sqrt{2\Pi}\sigma}e^{-(y_i - y)^2 \div \sigma^2}.\qquad(4)$$

A set of points were extracted and connected with a spline function into a smooth curve. Hereinafter the teeth gap valley detection is based on the sum of intensities of the perpendicular lines to the boundary. The tooth isolation is obtained through the previous step, *i.e.*, each pair of consecutive perpendicular lines contain a single tooth between them. The contour extraction is based in the probability of each pixel in the Region of Interest (ROI), which in this case corresponds to the isolated tooth, belonging to the ROI, starting from the center of the region targeted in the previous steps. Finally, the contour comparison is performed in order to obtain human identification. Despite the good results obtained by the authors, this method is very dependent on the users input as a wrong initialization point has the consequence of not yielding any segmented tooth.

1.5   Teeth Segmentation

Image segmentation is one of the most difficult tasks in image processing and it plays an important role in most subsequent image analysis, specially in pattern recognition and matching. Segmentation consists in the partitioning of an image into its constituent regions and in the extraction of the objects of interest. However, there is no any image segmentation technique that performs well in all problems. In addition, the performance of a segmentation technique is greatly affected by noise embedded in images.

In [16], authors performed the teeth segmentation in digitalized dental X-ray films using mathematical morphology, proposing new approach to the problem of identification of the PM through dental X-rays. Mathematical morphological method are used in the segmentation of teeth and a decrease in processing of contrast in grayscale to improve the segmentation problem. The ROI is a rectangular area in the original image containing a tooth. The three main rules for the extraction are, firstly the retrieving of the largest possible number of teeth, secondly only operate in bitewing and periapical X-rays and finally in the worst case extract at least one tooth per image. To perform the segmentation authors divided the grayscale range in three distinct regions: brighter areas which define

most teeth found in X-ray images, middle areas that correspond to the bones and finally the darker areas concerning the background.

The segmentation process is divided in four main stages, firstly the internal noise filtering that consists in the teeth gap valley detection and in the partitioning of the jaws. This step uses both horizontal and vertical projection of the sum intensities for the detection of the gap valley between the upper and the lower jaw based on the previous three defined distinct range regions of the grayscale. Secondly is the threshold operation, where the main goal is to divide the teeth from the background and the dental bones. Because of the shading effect present in the dental X-ray images, the extraction of only one threshold is not advisable. Therefore the extraction of three thresholds was performed, based on the cumulative histogram of the filtered images. Thirdly, is performed the connected components labeling [7][6], in this case there are four different types of connected components: a) the teeth that are considered as ROI, b) more than one tooth due to overlap, c) connected components corresponding to the background or bones and d) corresponding to parts of the teeth, such as root or crowns. Finally, is the refinement where the selection of the best candidates of the connected components is carried out.

1.6 Active Contours without Edges

Based on techniques of curve evolution, Mumford-Shah functional and level sets, the active contour without edges model [2] can detect objects whose boundaries are not necessarily defined by the gradient, in the level set formulation, the problem becomes a "mean-curvature flow" evolving the active contour, which will stop on the desired boundary. However, the stopping term does not depend on the gradient of the image, as in the classical active contour models, but is instead related to a particular image property. Assuming that a image ω_0 is composed by two related regions of approximately constant intensities, of distinct values, ω_0^i and ω_0^j. The object that we want to segment is represented by the values of ω_0^i and the boundary is denoted by C_0. Therefore when we are inside the object we have $\omega_0 \approx \omega_0^i$ or inside the object boundary (C_0), and $\omega_0 \approx \omega_0^j$ outside the object boundary. Defining the fitting term, given by the (5):

$$
\begin{aligned}
F_1(C) + F_2(C) &= \int_{inside(C)} |\omega_0(x,y) - c_1|^2 dxdy \\
&+ \int_{outside(C)} |\omega_0(x,y) - c_2|^2 dxdy
\end{aligned}
\tag{5}
$$

Where C is the variable curve, and the constants c_1, c_2, depending on C, are the intensities averages of ω_0 inside and outside C. In this case the fitting term is given by the boundary of the object C_0, as shown in (6):

$$
\inf_C \{F_1(C) + F_1(C)\} \approx 0 \approx F_1(C_0) + F_1(C_0).
\tag{6}
$$

For example, if the curve C is outside the object, then $F_1(C) > 0$ and $F_2(C) \approx 0$. If the curve C is inside the object, then $F_1(C) \approx 0$ but $F_2(C) > 0$. If the curve C is both inside and outside the object, then $F_1(C) > 0$ and $F_2(C) > 0$. Finally,

the fitting energy is minimized if $C = C_0$ *i.e.*, if the curve C is on the boundary of the object. Authors [2] minimized the fitting term and they also added some regularizing terms, such as the length of the curve C and the area of the region inside C, making the energy functional defined by $F(c_1, c_2, C)$, as shown in (7):

$$F(c_1, c_2, C) = \mu * Length(C) + \nu * Area(inside(C))$$
$$+\lambda_1 \int_{inside(C)} |\omega_0(x, y) - c_1|^2 dx dy \qquad (7)$$
$$+\lambda_2 \int_{outside(C)} |\omega_0(x, y) - c_2|^2 dx dy$$

where $\mu, \nu \geq 0$, $\lambda_1, \lambda_2 > 0$ are fixed parameters.

This technique of active contours is used in our work in two different stages: in the teeth gap valley detection and in the tooth segmentation.

2   Main Goal / Motivation

The main goal of the work presented here, is to detect dental caries in panoramic dental X-ray images, by signalling the infected teeth in the image. To the best of our knowledge, there is a lack of a complete case study in the literature, as only methods that describe parts of the whole process can be found. This work should interest the scientific community, as it can constitute a comparison term for other methods concerned with the detection of dental caries in panoramic X-ray images.
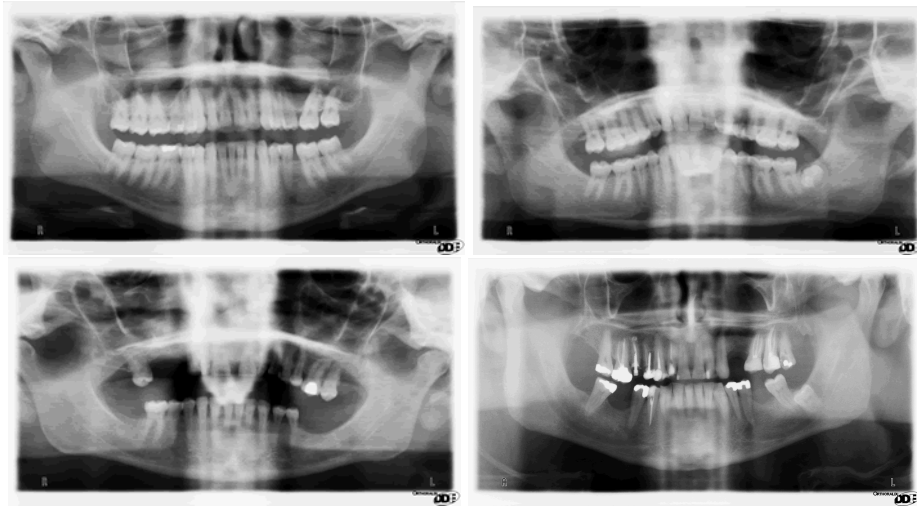
3   Data-Set

Images of our data-set were captured by an Orthoralix 9200 DDE X-ray camera. There are a total of 1392 grayscale images in the data set, with varying types of dental structures, mouth sizes and number of teeth per image, as can be seen in figure 1. Another major point of interest of this data set are maps that detect and localize dental cavities acting as ground truth of automated methods. Also, we believe that this set of images is useful to evaluate the current teeth segmentation methods.

3.1   Morphological Properties

When compared to other types of stomatology images, radiographic images are highly challenging, due to several reasons:

– Different levels of noise, due to the moving imaging device that captures a global perspective of the patient's mouth.
– Low contrast, either global or on local regions of the images. The dictated by the mouth topology and morphologic properties, which are very complex.
– The blurring that makes difficult the straightforward detection of edges.
– The noise originated by the spinal-column that covers the frontal teeth in some images, as shown in figure 1.

Fig. 1. Examples of images of the Dental X-ray data set.

4 Method

As show in figure 2, our work comprises four different stages. The first stage is based in a statistically analysis of the images morphology, in order to define a preliminary ROI that takes out the nasal and chin bones. Next, we make the detection of the upper jaw and the lower jaw, based on the extraction of primitive points between jaws and in the application of a polynomial fitting process to connect all the primitive points. The second stage is the teeth gap valley detection, where first we detect the gap valleys based in active contours techniques [2]. This process is applied in each jaw represented in the polar coordinate system. Secondly, we divide each tooth by extracting the points that are minimums in their contour neighborhood. The third stage consists in the accurate segmentation of each tooth. Here, we also used the active contours technique. Finally, we extract the dental features and classify dental caries. A large variety of features were used to feed our binary classifier: statistical, image characteristics, region based features, texture based features and features based on the tooth border.

4.1 ROI Definition

Our method starts by the detection of a ROI, that should contain the mouth and teeth and discard non-useful information, as the nasal and chin bones. This stage is based in a statistics of the sizes and positions of each component in each image. Having as purpose for each image we measured four distances (R_1, R_2, R_3, R_4), defined by $R_i = \sqrt{(x_c - x_{R_i})^2 + (y_c - y_{R_i})^2}$, where (x_c, y_c) corresponds to the image center $(x_c, y_c) = (w/2 = 1408, h/2 = 770)$ and (x_{R_i}, y_{R_i}) corresponds to the four points extracted from the left, right, upper and lower side of the mouth.
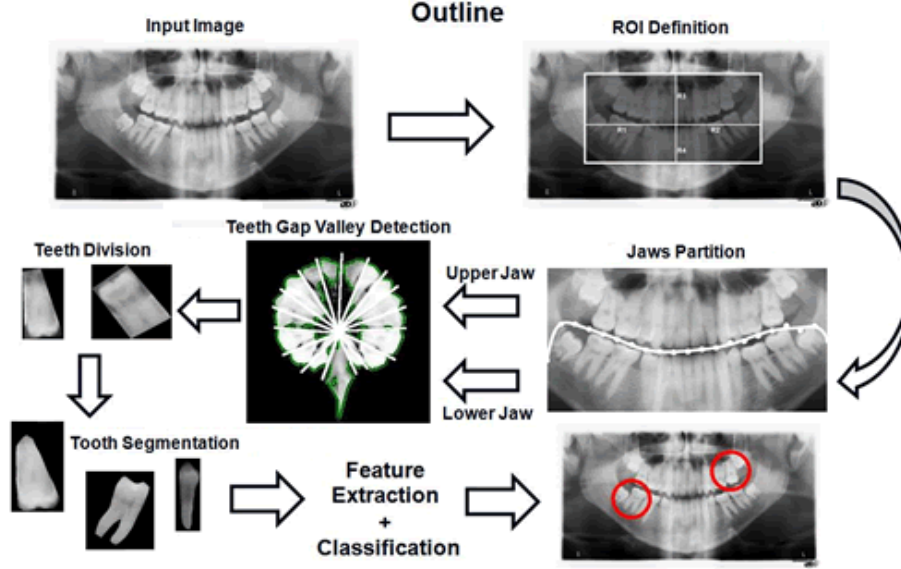
Fig. 2. The Outline of our developed work.

With this distances R_i we extract from our training set four histograms for each distance. The histograms of R_i enabled us to fit corresponding Gaussian distributions for each distance defined by their mean and standard deviation: (μ, σ). Based on these distributions, we obtained the minimum value for each R_i that would appropriately crop the data with 95% certainty. Furthermore, a margin guarantees that slightly different images will be appropriately cropped, even at the expresses of a small increment of useless regions. The values obtained were $R_1 \approx 897.77$, $R2 \approx 863.36$, $R3 \approx 406.31$, and $R4 \approx 471.27$.

4.2 Jaws Partition

This stage concerns about the partition of the jaws. Firstly, the extract points between the jaws and then connecting those points by a polynomial least squares fitting scheme, a derivation of the least squares fitting [15]. The set of points is obtained based on the horizontal projection $v(u)$ of the images, given by (8), where $I(x,i)$ denotes the intensity value at line x and column i:

$$v(u) = \sum_{i=0}^{w} I(x,i) \tag{8}$$

The initial point $p_0(x_0, w-1)$ is defined at the far right of the image and at the line that has the minimum $v(u)$ value:

$$p_0(x_0, w-1) = \arg\min_x(v(u)) \qquad (9)$$

where w is the image width and the remaining set of points p_i are regularly spaced, starting from $p_0 : p_i(x_i, (w-1) - W/21)$, where x_i is obtained similarly to x_0. To avoid too high vertical distances between consecutive p_i, we added the following constraints:

$$p_i(x_i, y_i) = \begin{cases} p_i(x_{i+1} + T, y_i), & | p_i(x_i, y_i) - p_{i+1}(x_{i+1}, y_{i+1}) | > T \\ p_i(x_i, y_i), & otherwise \end{cases} \qquad (10)$$

We empirically obtained $T = 20$, in order to avoid huge vertical distances, which plays a major role in dealing with missing teeth. Having the set of $p_i(x_i, y_i)$ primitive points, the division of the jaws is given by the 10th order polynomial, (11), obtained by a polynomial least squares fitting algorithm based on the Vandermond matrix:

$$p(x) = a_0 x^0 + \ldots + a_{10} x^{10} \qquad (11)$$

The performance of this stage depends on the number of the missing teeth present in the input image, specially when more than one consecutive tooth is missing.

### 4.3 Teeth Gap Valley Detection

Having booth jaws divided, the next goal is to detect the teeth gap valley. These valleys tend to be darker than the teeth themselves, although exceptions are due to teeth overlap. Our main concern was the tracing of lines that appropriately divide teeth. Starting by the transformation of our images from cartesian coordinates to polar coordinates which we used to easy the division between teeth, usually by radial lines. The next step is the contour segmentation, as we regard this stage as a typical active contours problem. Here the object of interest is in the center of the image and therefore the contour can be initializing as the image border. In the third step we calculate for each contour point the distance between the center of the image and based on their values, we extract the minimum points, which in this case correspond exactly to the teeth gap valleys. The final step corresponds to the crop of the output regions.

Morphological operators To increase the contrast of the input images we applied a pre-processing filter (top and bottom hat transform):

$$\begin{aligned} I_{output} &= (I_{Original} + TH_{Original}) - BH_{Original} \\ I_{outputFinal} &= (I_{output} + TH_{output}) - BH_{output} \end{aligned} \qquad (12)$$

where $I_{Original}$ corresponds to the input image, $TH_{Original}$ is the output of the top hat transform $BH_{Original}$ is the output bottom hat transform. The

resulting image of the pre processing filter is $I_{outputFinal}$. We used a rectangular structuring element with dimensions $[w/4, h/2]$, where w and h are the width and height of the image, respectively. This choice was based in a training set of 500 images, selected from the whole data set. As can be seen in the left column of the figure 3, pre processing increased the contrast of the image. A less successful example can be seen in the right column of the figure 3, where the pre processing of teeth contributed for the disappearing of the frontal teeth. This occurs only in these teeth, because they are thinner and can't reflect as much radiation as do the pre molars and molars. Other cases are due to the poor quality of the image. Jaws were divided simply by an horizontal and linear partition of the
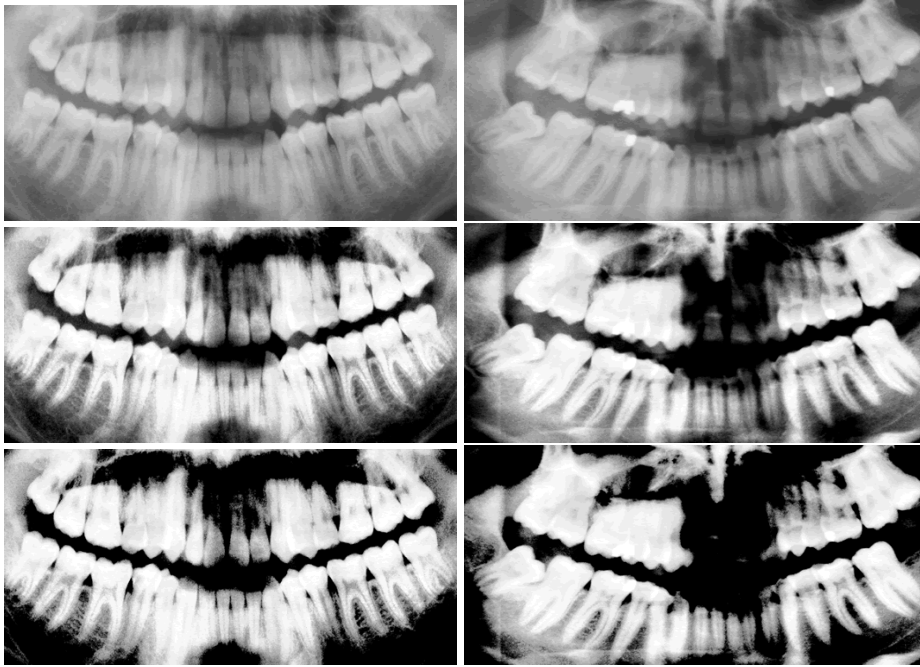
Fig. 3. Examples of a successful (left column) and failure (right column) cases of the pre-processing module.

image. The upper jaw was cropped in the lower value of the polynomial found in the previous stage. The lower jaw was cropped in the higher value that the polynomial takes.

Polar Coordinates In mathematics, the polar coordinate system is a two-dimensional coordinate system, where each point is defined by a distance to a fixed point and the angle from a fixed direction. The polar coordinates [1] r (the radial coordinate) and θ (the angular coordinate, often called the polar angle).

In equation 13 the method to transform an (x, y) point in polar coordinates is described.

$$r = \sqrt{x^2 + y^2}$$
$$\theta = \tanh \frac{y}{x} \tag{13}$$

Where $\tanh \frac{y}{x}$ corresponds to a two argument inverse tangent which takes the signs of x and y into account as to determine in which quadrant θ lies. The equation of a curve expressed in polar coordinates is known as a polar equation, and a plot of a curve in polar coordinates is known as a polar plot. The resulting images in polar coordinates, had the follow dimensions $[h * 2; h * 2]$, where h corresponds to the height of the original input image. With this transformation of coordinates it is thus possible to transform our problem, in a problem typical of active contours. One of the main reasons of the use of polar coordinates is in fact referred to the radial division that is possible to perform in this image representation. This allows us to better improve the result of the active contours and as a result the teeth division becomes an easier task.

Active contours without edges This segmentation method seeks for the minimization of an energy model, given by (7) and requires proper initialization of the contour mask. After the analysis of a training composed by 200 images we defined the initial mask corresponding to four independent elements in each image quadrant:

$$I_{mask}(x, y) = \begin{cases} ([w * 0.10...(w/2) * 0.90], [h * 0.10...(h/2) * 0.90]) = 255 \\ ([(w/2) + (w/2) * 0.10...w * 0.90], \\ \quad [h * 0.10...(h/2) * 0.90]) = 255 \\ ([(w/2) + (w/2) * 0.10...w * 0.90], \\ \quad [(h/2) + (h/2) * 0.10...h * 0.90]) = 255 \\ ([w * 0.10...(w/2) * 0.90], \\ \quad [(h/2) + (h/2) * 0.10...h * 0.90]) = 255 \end{cases} \tag{14}$$

where w and h correspond to the image width and height, respectively. With computational concerns we resized the input images by 0.25, giving data the size of $[w/4; h/4]$, where w corresponds to the width of the image in polar coordinates, and h is the value of the height input image in polar coordinates. In this case w and h are given by $h_{Original} * 2$, where $h_{Original}$ is the corresponding height of the image in cartesian coordinates.

4.4 Teeth Division

The division is based on the minimums extracted in the previous step:

- Let $c_1, ..., c_n$ be the set of contour points, where $c_i = (x_i, y_i)$. Let (x_c, y_c) be the image center. Let d_i be the distances between the center and the contour, i.e., $d^1 = \sqrt{(x_1 - x_c)^2 + (y_1 - y_c)^2}$.
- Let $D_i = d_i, ..., d_n$ corresponding to the distances vector. We eliminated all distances based on $d_i^2 = D_i \cap (A_1^{-1})$ where $A_1 = [D_i < 0.10 * h]$ where h corresponds to the height of the input image.

- After that we apply a Gaussian filter in order to smooth the output distances. Let $d_i^3 = d_i^2 \otimes G_{\sigma,r}$ where $G_{\sigma,r}$ is a Gaussian Kernel[17][13] of sigma $\sigma = 10$ and radius $r = 100$.
- Defining d_i^m as the local minimums extracted from d_i^3, *i.e.*, $d_i^m = (((d_i^3(x - 3) > d_i^3(x - 2) > d_i^3(x - 1)) > d_i^3(x))$ && $(d_i^3(x) < d_i^3(x + 1)))$ where x corresponds to the indices vector in analysis.

The final step consists in the extraction of a neighbor second point, based on the line that is performed by the extracted point and the image center and taking in consideration the intensity similarity. With this second point we calculate the correspondent coordinates in the cartesian system, allowing the drawing of the line and the region cut for each extracted tooth. As shown in the figure 4 the

**Fig. 4.** An example of our method for the teeth gap valley detection.

extraction of the minimum is very dependent on the coordinates transitions, because it is inherent a loss of information in such transitions. Which leads to the cutting of some teeth demonstrating that some improvements need to be carried out. It is also important to highlight the non-detection when the teeth overlap is strong, thus not enabling the detection of teeth gap valleys.

4.5 Tooth Segmentation

This process is quite similar to the teeth gap valley detection stage. The input images contain only one tooth and the problem is to distinguish between teeth and background corespondent to the gum line and the gum itself. The pre-processing was similar to the one applied earlier in the Teeth Gap Valley Detection stage. As shown in the figure 5 the application of the active contours technique appears to have been a very good option. It should be stressed that all segmented regions actually the tooth, *i.e.* the region corresponding to the tooth is always inside the resulting region, although sometimes due together with some background noise. In other cases, overlap teeth leaded to the inclusion of multiples teeth in the segmented region as shown in figure 5.

4.6 Dental Caries Classification

This stage starts by the extraction of features which apriority could carry relevant information to the problem. To do this we created a training set of 1098
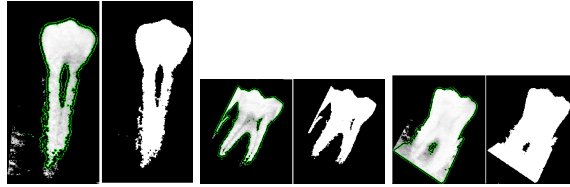
Fig. 5. Examples of the active contours method applied to our input images.

images, with 549 images with dental caries and 549 images containing healthy teeth. This training set contains all types of teeth, but with pre molars and molars in majority due to a similar proportion in the available data set. We use different types of features, hence the importance of using algorithms for selecting the best features, which we choose to use the PCA algorithm. As the number of extracted features was very large, we further reached the features space dimensionality, with the PCA method. These features consist in five groups:

1. Features based on the image characteristics; such as pixel intensity, maximum pixel intensity, etc.
2. Statistic features as the entropy, mean-value, variance and more.
3. Region based features such as the Hu moments, the Zernike moments, area, perimeter, etc.
4. Features based on the region segmented boundary, like chain code, Fourier descriptors, signature, angular function, among others.
5. And features based on the image texture, as the energy, third moment.

Table 1 show the types of features contain 95% and 99% of the total variance in the training set, according to each of the above defined types. The "Variance" column gives the percentage of features of the corresponding type that were selected by the PCA. "Number Features" gives the total number of features selected. It can be seen that the features based on the region boundary and the region itself had a significant preponderance when compared with other types of features. In turn, features based on the image properties do not add too much information to the feature set. Note also that the statistical features based on the boundary and the region correspond to a significant portion of the resulting set by the PCA algorithm.

5 Results

5.1 Segmentation

In this section we discuss the results of all the stages of our work. Starting with a few observations regarding the way these results were obtained as well as the sets we defined. For the ROI definition, jaws partition, teeth gap valley detection and tooth segmentation stages ground truth was given by visual inspection, with a 2-folder cross validation. It should be stressed that all the results were

Table 1. Results from applying the PCA in our initial feature set.

Features Based On	Variance 95% (%)	Number Features 65	Variance 99% (%)	Number Features 128
Image properties	6.1	4	3.1	4
Region	97	63	93.75	120
Boundary	100	65	100	128
Texture	46.2	30	39	50
Statistical	93	60	92.2	118

based on an error-free inputs from previous stages. This was performed in order ti avoid that errors in the earliest stages corrupt the results obtained by the final ones. Table 2 shows the results obtained by the first three stages of our method. As explained above, the results were obtained by visual inspection and the evaluation of our method is based on a completely separately set and through 2-folder cross validation. Results in the ROI definition and in the jaws partition

Table 2. Results of our method stages up to the Dental Caries Detection.

Stages	Results (% of correct)	Number of Images
ROI Definition	95.7	700
Jaws Partition	92.6	700
Teeth Gap Valley	87.5	700
Tooth Segmentation	71.91	1098

are quite satisfactory, which corresponds to an accuracy above 90% for a set of 700 images. For these two steps and concerning the visual inspection we consider as *correct* the presence of all teeth in the output image resulting of the ROI definition. Regarding the jaws partition we considered *correct* any polynomial that divides each jaw without cutting any tooth.

5.2 Classification

Feature normalization a necessary step because in many situations the features values lie within different dynamic ranges. Thus, features with large values may have larger influence in the cost function than features with small values, although this does not necessarily reflect their respective significance in the design of the classifier. The problem was solved by the normalization of the features, so their values lie within similar ranges. A straightforward technique is the normalization to save mean and variance. Other linear techniques limit the features value in the range of [0, 1] by proper scaling. We empirically evaluated each of the above described strategies.

Artificial Neural Network A feed-forward artificial Neural Network (NN) was used for classification proposes. Table 3 contains the best result obtained

for the test set, after the PCA with the covered variance of 99% and in figure 6 we show the correspondent Receiver Operating Characteristic (ROC) curve. As we can observe, the results can be considered satisfactory. Also, there is an increase of the accuracy rating after the appliance of the PCA for a 99% variance coverage, which denotes the importance of the attributes selection performed by the PCA. Another conclusion drawn from these results is that extracted features

Table 3. Confusion matrix for the ANN classifier for the normalized test set between [0, 1] after the appliance of the PCA for a 99% variance coverage.

Class	No Dental Caries	Dental Caries	Total
No Dental Caries	548	1	549
Dental Caries	13	536	549
Total	561	537	1084
Accuracy	98, 70%		
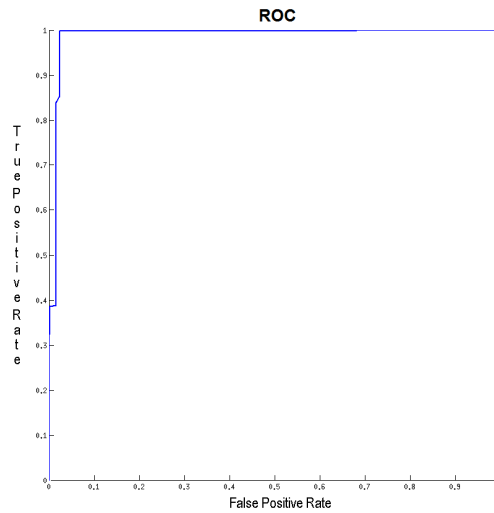
Fig. 6. ROC for the ANN classifier for the normalized test set between [0, 1] after the appliance of the PCA for a 99% variance coverage.

have enough discriminating capacity to decide with high confidence whether a tooth contains or not a dental cavity.

6   Conclusion

The main contribution of this work is the development of a complete case study for the dental caries detection in dental panoramic X-ray. Also, announced the availability of a new data set of panoramic dental X-ray images, which can constitute a tool for the research community in the development of stomatologic-related applications. This data set has varying morphologic properties that make it valuable to the scientific community. These include the number of teeth per image, the shape of the mouth and teeth as well as the levels of noise. Concerning the first two stages of the proposed method the results were considered satisfactory, obtaining in the ROI definition a accuracy of 95.7% and in the jaws partition a result of 92.6%. The other three stages had the accuracy rating of 87.5% (teeth gap valleys detection) and 71.91% (tooth segmentation). Finally, the accuracy of the classification module was 98.70%. These results regard each stage independently, which enabled us to perceive the actual merits of each module without corruption of the results due to errors in previous stages.

7   Future Work

In the jaws partition as future work, it is very important to detect missing teeth because in these situations our algorithm tends to not compensate the missing teeth present in the input image, for example detect if the polynomial extracted has in the various stripes equally mean-values intensities. In a strip where this propriety is not fulfilled we are over a brighter area of the image, and possibly a tooth.

In the teeth gap valleys detection dividing the image in three different zones (left, frontal and right) for the correct appliance of the top and bottom hat transform. The improvement concerning the teeth overlap, applying local erosion in brighter areas, that in most cases corresponds to teeth overlap zones.

Finally as future work our main goal is to start the detection of other types of dental diseases, using the described dental X-ray data set. For now we are starting by the detection of dental cavities in the future hopefully move to other types of pathologies.

References

1. Howard A. Anton, Irl Bivens, and Stephen Davis. *Calculus*. Wiley, 7th edition, 2001.
2. Tony F. Chan and Luminita A. Vese. Active contours without edges. *Image Processing, IEEE Transactions*, 10:266–277, 2001.
3. Hong Chen and Anil K. Jain. Matching of dental x-ray images for human identification. *Pattern Recognition*, 37:1519–1532, 2004.
4. Hong Chen and Anil K. Jain. Tooth contour extraction for matching dental radiographs. *17th International Conference on Pattern Recognition (ICPR'04)*, III:522–525, 2004.

5. Nello Cristianini and Jonh Shawe-Taylor. *An Introduction to Support Vector Machines and Other Kernel-based Learning Methods.* Cambridge University Press, 1st edition, 2002.

6. E. R. Davies. *Machine Vision: Theory, Algorithms, Practicalities.* Morgan Kaufmann Publishers Inc., 3rd edition, 2005.

7. Rafael C. Gonzalez and Richard E. Woods. *Digital Image Processing.* Prentice-Hall, 3rd edition, 2008.

8. Anil Jain, Lin Hong, and Sharath Pankanti. Biometrics: promising frontiers for emerging identification market. *Communications of the ACM*, pages 91–98, 2000.

9. I.T. Jolliffe. *Principal Component Analysis.* Springer Series in Statistics, 2nd edition, 2002.

10. Shuo Li, Thomas Fevens, Adam Krzyak, Chao Jin, and Song Li. Semi-automatic computer aided lesion detection in dental x-rays using variational level set. *Pattern Recognition*, 40:2861–2873, 2007.

11. Shuo Li, Thomas Fevens, Adam Krzyzak, and Song Li. An automatic variational level set segmentation framework for computer aided dental x-rays analysis in clinical environments. *Computerized Medical Imaging and Graphics*, 30:65–74, 2006.

12. David Meyer, Friedrich Leisch, and Kurt Hornik. The support vector machine under test. *Image Processing, IEEE Transactions*, 55:169–186, 2003.

13. Mark S. Nixon and Alberto S. Aguado. *Feature Extraction and Image Processing.* Newnes, 1st edition, 2002.

14. HyunWook Park, Schoepflin T., and Yongmin Kim. Active contour model with gradient directional information: directional snake. *Circuits and Systems for Video Technology, IEEE Transactions*, 11:252–256, 2001.

15. Dyer S.A. and Xin He. Least-squares fitting of data by polynomials. *IEEE Instrumentation and Measurement Magazine*, 3:46–51, 2001.

16. Eyad Haj Said, Diaa Eldin M. Nassar, Gamal Fahmy, and Hany H. Ammar. Teeth segmentation in digitized dental x-ray films using mathematical morphology. *IEEE Transactions on Information Forensics and Security*, 1:178–189, 2006.

17. Linda G. Shapiro and George C. Stockman. *Computer Vision.* Prentice-Hall, 1st edition, 2001.